Hindawi
Shock and Vibration
Volume 2019, Article ID 7463031, 12 pages
https://doi.org/10.1155/2019/7463031

Research Article

Effect of SSI on Vibration Control of Structures with Tuned Vibration Absorbers

Said Elias [1,2]

[1]*Earthquake Engineering Research Centre, University of Iceland, Reykjavík 101, Iceland*
[2]*Department of Civil Engineering, Herat University, Herat, Afghanistan*

Correspondence should be addressed to Said Elias; eliasrahimi959@gmail.com

Received 9 November 2018; Accepted 2 January 2019; Published 23 January 2019

Academic Editor: Marco Belloli

This paper investigates the effect of considering soil-structure interaction (SSI) in seismic responses of reinforced concrete (RC) chimneys installed by distributed tuned vibration absorbers vertically (d-MTVAs). A multimode control approach is used to design the d-MTVAs. Two-dimensional (2D) RC chimney is the assembly of beam elements. Frequency-independent constants for the springs and dashpots are used for modeling the raft and the surrounding soil. The equations of motion for nonclassically damped systems are derived and solved using Newmark's method. The effectiveness of the d-MTVAs is weighed against the case of single tuned vibration absorber (STVA), d-MTVAs suppressing the first modal responses (d-MTVAs-1), and randomly distributed MTVAs (ad-MTVAs). Additionally, parametric studies are conducted for varying mass and damping ratios in the STVA, d-MTVAs-1, ad-MTVAs, and d-MTVAs. In order to show the efficiency in the STVA, d-MTVAs-1, ad-MTVAs, and d-MTVAs cases, responses (displacement and acceleration) at top of the RC chimney while subjected to different real earthquake excitations are computed. It is concluded that the STVA, d-MTVAs-1, ad-MTVAs, and d-MTVAs are effective in response mitigation of the RC chimney; however, d-MTVAs are more efficient while considering equal total mass of the TVA(s). Moreover, the soil type significantly influenced the design parameters of the STVA/d-MTVAs-1/ad-MTVAs/d-MTVAs and seismic response of the RC chimney.

1. Introduction

Industries generally used reinforced concrete (RC) chimneys with varied geometries. Earthquake forces caused damages or collapses to several chimneys. Kocaeli earthquake in 1999 and Chile earthquake in 2010 are the examples which caused collapses to the RC chimney. The design of chimneys is a well-established procedure for working engineers and researchers. Many of the researchers believe that if the chimney is considered to be located in a location with medium to soft soil, the modeling will depend on the type of foundation. In such a site, the structure will be supported on very deep foundation if the rock is too deep or it will be supported on a combination of mat foundation and deep foundation (where part of the site is reinforced using piles) or it will be supported on rock-socketed piles or drilled shafts. The researchers believe that if the chimney is modeled with these foundations, then the behavior of such foundations will be mobilized because of dynamic loads; i.e., there will not be much soil-structure interaction (SSI) under dynamic loads. Hence, many of them ignored the effect of SSI in their studies [1–4]. The other researchers such as Solari and Stura [5], Arunachalam et al. [6], and Chmielewski et al. [7] have included the effect of the SSI in dynamic analysis of structures. Tuned vibration absorber (TVA) is one such conventional passive mechanism, which consists of a mass, a spring, and a viscous absorber installed on the main structure in order to mitigate any adverse vibrations. Researchers such as Kareem [8], Aly et al. [9], Aly [10, 11], Roffel and Narasimhan [12], and Elias and Matsagar [13] had employed the TVA in structures and reported reasonably enhanced vibration response control in the structures. However, single TVA is reported to be less efficient due to off-tuning. Therefore, the researchers [14–18] suggested to use multiple TVAs (MTVAs) in order to fix the issue of the off-tuning. Guo et al. [19] found that the nonlinear TMD is more applicable to determine excitation, like wind. However, the difficulty of adding massive mass on a particular

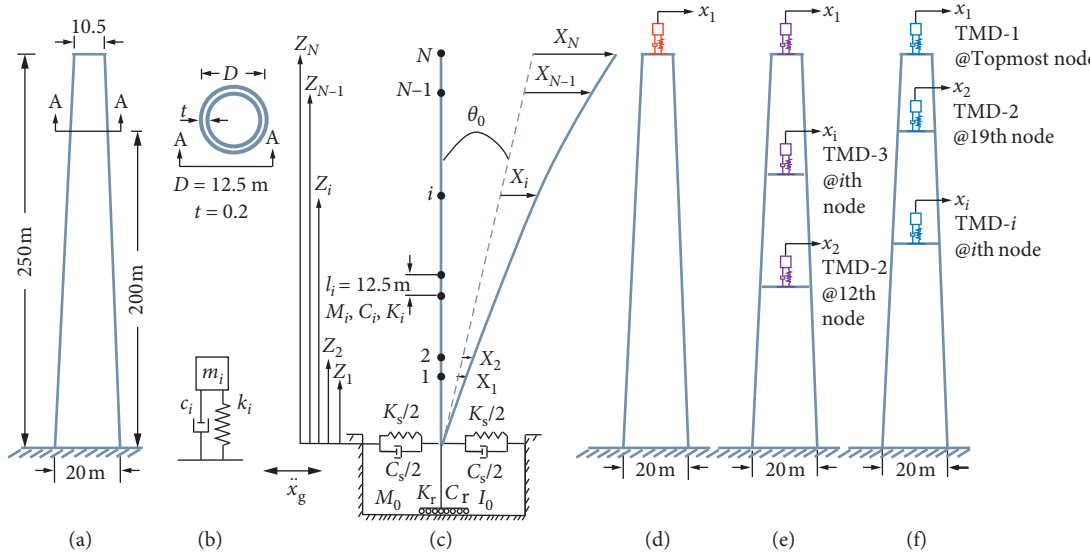

FIGURE 1: (a) Details of the chimney with no control, i.e., uncontrolled (NC); (b) schematic diagram of TVA and section A-A; (c) lumped mass idealization for the chimney including SSI and installed with (d) STVA, (e) ad-MTVAs, and (f) d-MTVAs.

elevation of the structure counted to be an important issue. The latest well-designed procedure is made for MTVAs to vertically distribute them (d-MTVAs). The d-MTVAs are used for vibration control of different types of structures under different loading conditions [20–24]. Tong et al. [25] demonstrated how to optimally tune the TMDs to reduce vibrations of flexible structures. Zaafouri et al. [26] designed a discrete-time sliding mode control using the equivalent discrete time reaching law for response control of structures. However, no study is conducted on earthquake response control of the chimney wherein placement and tuning of the d-MTVAs are made in accordance with the chimney including SSI. The objective of the present study is to study the efficient positioning and tuning of the d-MTVAs based on the modal properties of the fixed-base uncontrolled chimney. In this technique, TVA(s) is(are) located where the normalized amplitude of the mode shape of the chimney is the highest or higher in the particular mode shape and the TVA(s) is(are) tuned to the matching modal frequency. Hence, the d-MTVAs are located to suppress the first few selected modal responses of the RC chimney including SSI. With the intention of showing the efficiency of the d-MTVAs located based on modal properties of the chimney, the seismic responses are achieved using (i) single tuned vibration absorber suppressing only the first modal responses (STVA), (ii) d-MTVAs suppressing the first modal responses (d-MTVAs-1), and d-MTVAs located randomly (ad-MTVAs). Moreover, a comprehensive parametric study is performed to discover the parameters which influence the response mitigation under the real seismic ground motions.

2. Modeling of Tall Chimney with SSI

The beam elements are assembled to model the chimney with sway degrees of freedom (DOFs). The DOFs are considered to be the dynamic degrees of freedom of the chimney with consideration of the soil-structure interaction (SSI). The hypothetical modeling is based on the hypothesis that the cross-sectional dimension in the element residue is the same. More hypotheses prepared for the systematic formulation are as follows: (i) the chimney is measured to stay in the elastic boundary under earthquake excitations and (ii) each scheme is considered to be under a single horizontal (unidirectional) component of the earthquake ground motion. Figures 1(a)–1(f) show N-degree-of-freedom (DOF) chimney equipped with n-DOF TVAs and two DOFs considered by SSI effect. For each node of the chimney, M_i is the mass, while I_i is the moment of inertia, and those of the foundation are shown as M_0 and I_0, respectively. K_i and C_i are, respectively, assumed to be the stiffness and damping between the nodes. The ith TVA contains mass (m_i), stiffness (k_i), and damping (c_i). Stiffness of the swaying and rocking springs is represented as K_s and K_r, and the damping of the corresponding dashpots is indicated as C_s and C_r, respectively. The differential equation of motion for the coupled system considered is obtainable using

$$[M_s]\{\ddot{x}_s\} + [C_s]\{\dot{x}_s\} + [K_s]\{x_s\} = -[M_*]\{r\}\ddot{x}_g, \quad (1)$$

where $[M_s]$ is the mass matrix, whereas the damping and stiffness matrices of order $(N+n+2)\times(N+n+2)$ of the chimney are $[C_s]$ and $[K_s]$, respectively. Furthermore, the unknown relative nodal displacement, velocity, and acceleration vectors are, respectively, $\{x_s\} = \{X_1, X_2, \cdots, X_{N-1}, X_N, x_1, \cdots, x_n, \theta_0, X_0\}^T$, $\{\dot{x}_s\}$, and $\{\ddot{x}_s\}$. The acceleration mass matrix for the earthquake is $[M_*]$, the earthquake ground acceleration is represented by $\ddot{x}_g$, and $\{r\}$ is the vector of influence coefficients.

Many of the standards such as the Indian standard or the Chilean code supervision indicate that 90% or above of the modal mass has to be taken into consideration for dynamic analysis. Therefore, for the present study, the author decided

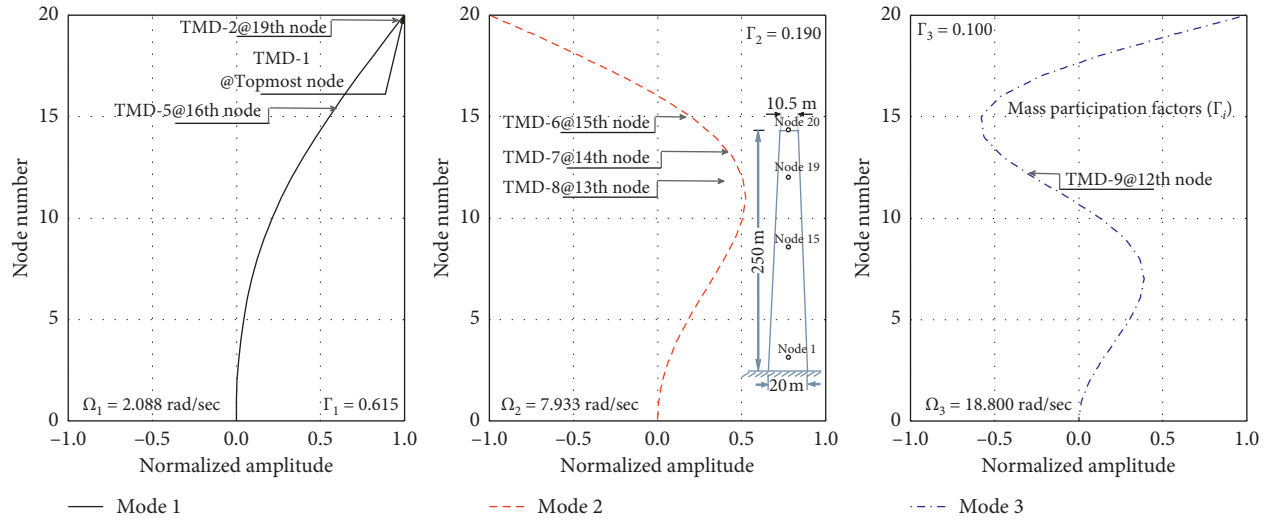

Figure 2: Mode shapes and frequencies of the uncontrolled chimney.

that the controlled modal responses should have modal mass greater than or equal to 90%. The first three modal responses of the chimney are controlled by installation of STVA, d-MTVAs, ad-MTVAs, and d-MTVAs. The mass participation factors for the first mode, for the second mode, and for the third mode are 0.615, 0.190, and 0.100, respectively. Thus, it is decided to have more number of TVAs to control the first modal responses as compared to the number of TVAs for second and third modal responses. The modal frequencies and mode shapes of the chimney with placement of the 9d-MTVAs are shown in Figure 2. The total number of TVAs n is measured to be 9, which 5d-MTVAs installed for suppressing the first modal responses, 3d-MTVAs installed for suppressing the second modal responses, and single TVA installed for suppressing the third modal responses. The performance of the 9d-MTVAs is compared with that of other TVA schemes such as STVA, 9d-MTVAs-1, and 9ad-MTVAs.

The mass ($[M_s]$), acceleration mass ($[M_*]$), damping ($[C_s]$), and stiffness ($[K_s]$) matrices are of order $(N+n+2)\times(N+n+2)$ and given as follows:

$$[M_s] = \begin{bmatrix} [M_N]_{N\times N} & [0]_{N\times n} & [M_N]_{N\times 1} & [M_N Z_N]_{N\times 1} \\ [0]_{n\times N} & [m_n]_{n\times n} & [m_n]_{n\times 1} & [m_n Z_n]_{n\times 1} \\ [M_N]_{1\times N} & [m_n]_{1\times n} & M_0 + M_t + m_t & \sum_i^N M_i Z_i + \sum_i^n m_i Z_i \\ [M_N Z_N]_{1\times N} & [m_n Z_n]_{1\times n} & \sum_i^N M_i Z_i + \sum_i^n m_i Z_i & I_0 + \sum_{i=1}^N I_i + M_i Z_i^2 + \sum_i^n m_i Z_i^2 \end{bmatrix},$$

$$[M_*] = \begin{bmatrix} [M_N]_{N\times N} & [0]_{N\times n} & 0 & 0 \\ [0]_{n\times N} & [m_n]_{n\times n} & 0 & 0 \\ 0 & 0 & M_0 + M_t + m_t & 0 \\ 0 & 0 & \sum_i^N M_i Z_i + \sum_i^n m_i Z_i & 0 \end{bmatrix}, \tag{2}$$

$$[C_s] = \begin{bmatrix} [C_N]_{N\times N} + [c_n]_{N\times N} & -[c_n]_{N\times n} & [0]_{(N+n)\times 1} & [0]_{(N+n)\times 1} \\ -[c_n]_{n\times N} & [c_n]_{n\times n} & 0 & 0 \\ [0]_{1\times(N+n)} & 0 & K_s & 0 \\ [0]_{1\times(N+n)} & 0 & 0 & K_r \end{bmatrix},$$

$$[K_s] = \begin{bmatrix} [K_N]_{N\times N} + [k_n]_{N\times N} & -[k_n]_{N\times n} & [0]_{(N+n)\times 1} & [0]_{(N+n)\times 1} \\ -[k_n]_{n\times N} & [k_n]_{n\times n} & 0 & 0 \\ [0]_{1\times(N+n)} & 0 & K_s & 0 \\ [0]_{1\times(N+n)} & 0 & 0 & K_r \end{bmatrix},$$

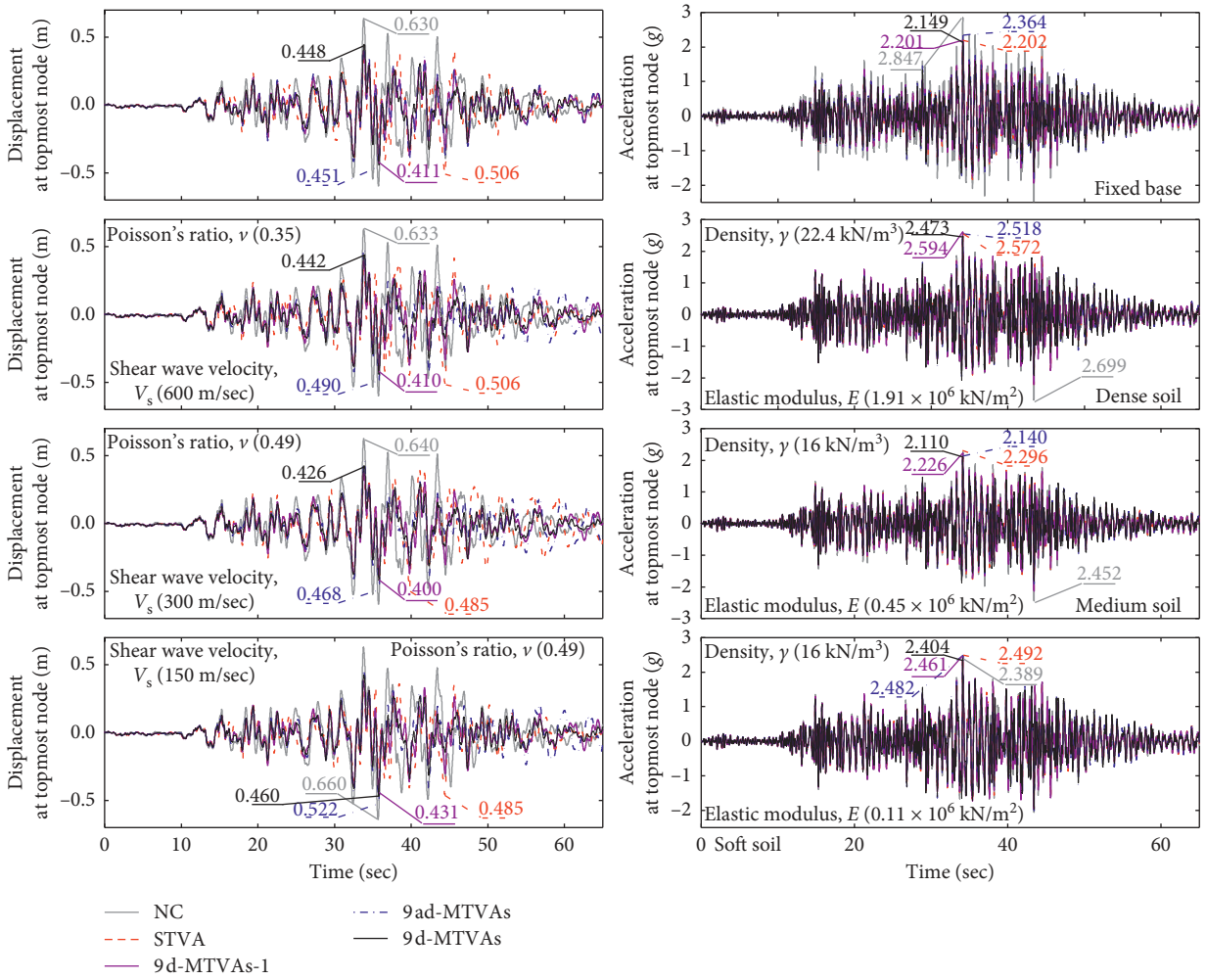

FIGURE 3: Time variation of displacement and acceleration at the topmost node of the chimney under Llolleo (1985); TVAs are with the mass ratio (μ) of 2% and damping ratio (ζ_d) of 5%.

where Z_i ($i = 1$ to N) is the height of the Nth node of the chimney and Z_i ($i = 1$ to n) shows the height of the nth TVA installed. $[M_N]_{N\times N}$ shows the mass matrix of the chimney, and $[m_n]_{n\times n}$ indicates the mass matrix of the TVAs. $m_t = \sum_{i=1}^{i=n} m_i$ is the total mass of the TVAs, and $M_t = \sum_{i=1}^{i=N} M_i$ is the total mass of the chimney. The TVAs are modeled by assuming that the mass is equally divided $m_i = m_t/n$. Natural frequencies of the d-MTVAs-1, ad-MTVAs, and d-MTVAs are uniformly distributed around their average frequencies. The natural frequency of each TVA (ω_i) is expressed by

$$\omega_i = \omega_T \left[1 + \left(i - \frac{n+1}{2}\right)\frac{\beta}{n-1}\right], \quad i = 1 \text{ to } n, \tag{3}$$

$$\omega_T = \sum_i^n \frac{\omega_i}{n}, \tag{4}$$

$$\beta = \frac{\omega_n - \omega_1}{\omega_T}, \tag{5}$$

where ω_T is the average frequency of all d-MTVAs-1/ad-MTVAs/d-MTVAs and β is the nondimensional frequency bandwidth of the d-MTVAs/ad-MTVAs/d-MTVAs systems. The stiffness (k_i) is used for adjusting the frequency of each TVA unit such that

$$k_i = m_i \omega_i^2, \quad i = 1 \text{ to } n. \tag{6}$$

The damping ($c_1 = c_2 = \cdots c_n$) of the TVAs is kept the same, and the damping ratio (ζ_i) of the TVAs is calculated as follows:

$$\zeta_i = \frac{c_i}{2 m_i \omega_i}. \tag{7}$$

Tuning frequency ratio (f) of the STVA/d-MTVAs-1/ad-MTVAs/d-MTVAs system is expressed as

$$f = \frac{\omega_T}{\Omega_N}, \tag{8}$$

where Ω_N is the natural frequency of the main chimney. The same procedure (equations (3)–(8)) is used for calculation of the MTVAs parameters in which their average tuning frequencies are the second and third frequencies of the chimney. STVA is always placed at the topmost node of the

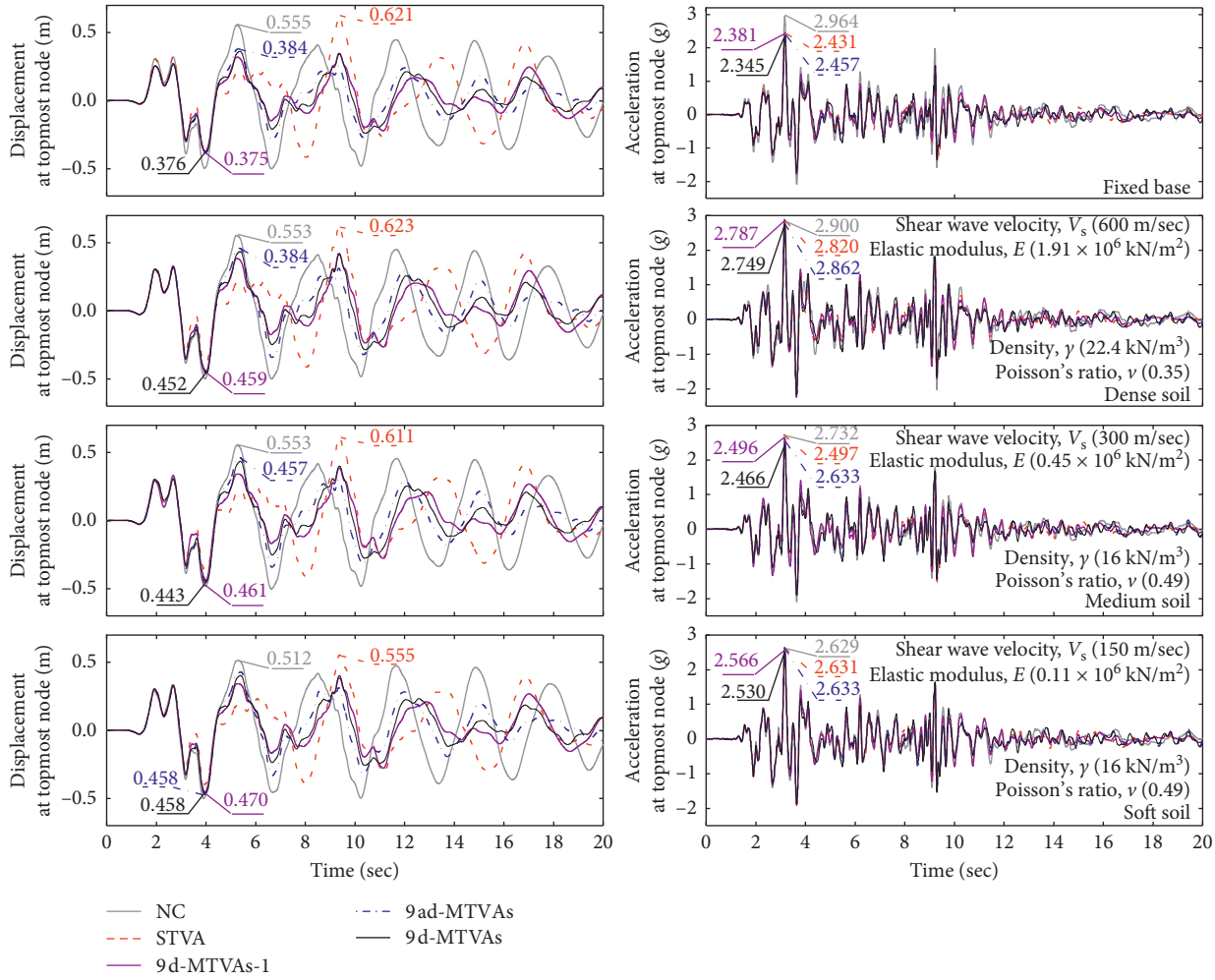

FIGURE 4: Time variation of displacement and acceleration at the topmost node of the chimney under Nahanni (1985); TVAs are with the mass ratio (μ) of 2% and damping ratio (ζ_d) of 5%.

chimney and tuned to the fundamental frequency of the chimney. The eigen vectors of the natural frequencies of the fixed-base uncontrolled chimney are estimated to do the placement of the d-MTVAs. In this procedure, the d-MTVAs controlling only fundamental modal responses are attached. Subsequently, the placement of the d-MTVAs controlling the second modal responses is attached, and finally, the last single TVA controlling the third modal responses is attached. It should be mentioned that there is only one TVA placed at a node. The subsequent TVAs are placed as per the criteria of the amplitude of larger to large in a particular mode.

3. Numerical Study

In this study, the RC chimney properties are taken from the model investigated by Datta and Jain [4]. This chimney is 250 m high and subjected to earthquake ground motion. The chimney is divided into 20 beam elements, and the length (l_i) of each beam element is 12.5 m. The chimney is having 20 degrees of freedom, and only the first three modal responses are controlled because 90% of the seismic mass is participating within the first three modes. The outer diameters (D), from the base to the top of the chimney, are 20 m, 19.5 m, 19 m, 18.5 m, 18 m, 17.5 m, 17 m, 16.5 m, 16 m, 15.5 m, 15 m, 14.5 m, 14 m, 13.5 m, 13 m, 12.5 m, 12 m, 11.5 m, 11 m, and 10.5 m, respectively. The corresponding thicknesses (t) are 0.85 m, 0.6 m, 0.55 m, 0.5 m, 0.45 m, 0.4 m, 0.35 m, 0.3 m, 0.25 m, 0.24 m, 0.23 m, 0.22 m, 0.21 m, 0.2 m, 0.2 m, 0.2 m, 0.2 m, 0.2 m, and 0.2 m, respectively. It is assumed that 2.5×10^{10} N/m^2 is the modulus of elasticity (E_c) of the concrete, and density of the concrete is considered 2,400 kg/m^3. Rayleigh's approach is used to calculate the damping matrix because the damping matrix is not explicitly known. In this method, the damping ratio (ζ_d = 5%) in all modes of vibration is considered. The STVA is installed on top of the chimney as shown in Figure 1(d). Arbitrarily distributed multiple tuned vibration absorbers (ad-MTVAs) installed along the height of the chimney are indicated in Figure 1(e). It is to be noted that, in the ad-MTVAs, the placement of TVAs along the height of the chimney did not follow any criteria. Furthermore, the chimney installed with the distributed multiple tuned vibration absorbers as per the modal properties of the chimney (d-MTVAs) is shown in Figure 1(f). The placement of the d-MTVAs-1 is exactly the same as that of the case of d-MTVAs. They fully control the

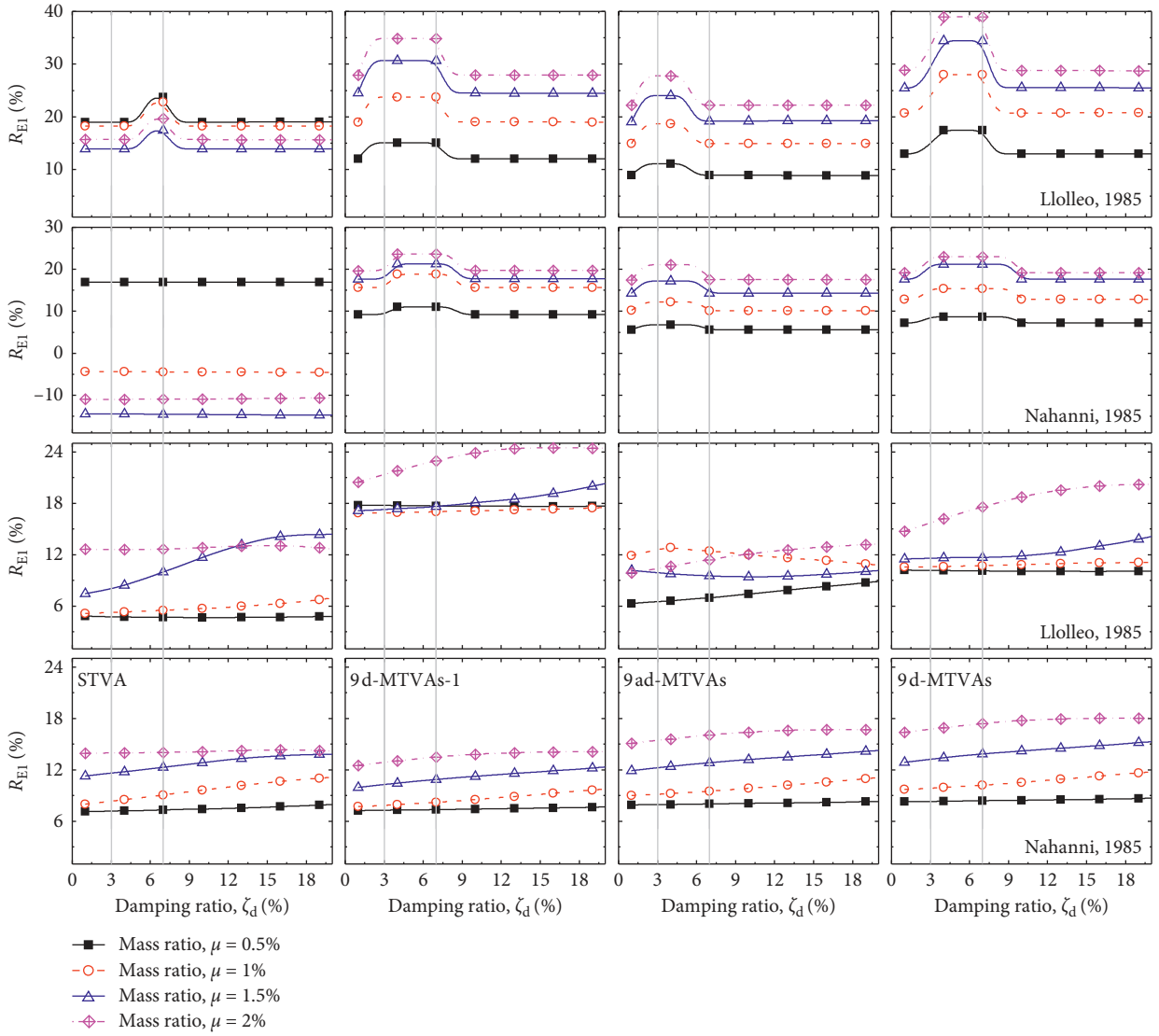

FIGURE 5: Variations of damping ratios (ζ_d) for different mass ratios (μ) of the STVA, 9d-MTVAs-1, 9ad-MTVAs, and 9d-MTVAs installed on the chimney with the fixed base under different earthquake ground motions.

fundamental modal responses. The mass participation factors (Γ_i) for the first, second, and third vibration modes are about 0.615, 0.190, and 0.100, respectively. The first three natural frequencies of the fixed-base uncontrolled chimney are $\Omega_1 = 2.088$ rad/sec, $\Omega_2 = 7.933$ rad/sec, and $\Omega_3 = 18.800$ rad/sec, which are the average tuning frequencies (ω_{T1}, ω_{T2}, and ω_{T3}) for the 5d-MTVAs-1, 3d-MTVAs-2, and d-MTVAs-3, respectively, controlling first, second, and third modes. The number of TMDs is chosen from the mass participation factor. Therefore, $n = 9$ is considered such that around 56%, 33%, and 11% mass of TMDs is used, respectively, for controlling the fundamental, second, and third modal responses. The placement of the nine TVAs (9d-MTVAs) in the scheme of the d-MTVAs is shown in Figure 2. Note that only one TVA is placed on the same node, while the placement of the TVAs is in accordance with the largest or larger amplitude of the mode shape, which would ease installation intricacies of the TVAs.

The soil is represented in a single layer under the footings, which consist of annular raft footing with the inner and outer diameter of 15 m and 40 m, respectively, and with the height of 2.5 m. The raft footing and the neighboring soil are modeled taking into account the springs and related dashpots as shown in Figure 1(c). The effect of considering different soil types is also investigated. The rock, dense soil, medium soil, and soft soil are, respectively, having the shear wave velocity (V_s) of 1200 m/sec, 600 m/sec, 300 m/sec, and 150 m/sec. In addition, Figures 3–9 contain the elastic modulus (E), density (γ), and Poisson's ratio (υ). Seismic response of the chimney is investigated under two real earthquake ground motions. Two historical earthquakes (Llolleo at station LLO in Chile and Nahanni at 6097 Site 1 in Canada) are taken as input excitation (m/sec^2) to evaluate the seismic performance of the chimney with the proposed control strategies. The peak ground acceleration (PGA) for the Llolleo (1985) and Nahanni (1985) earthquake ground

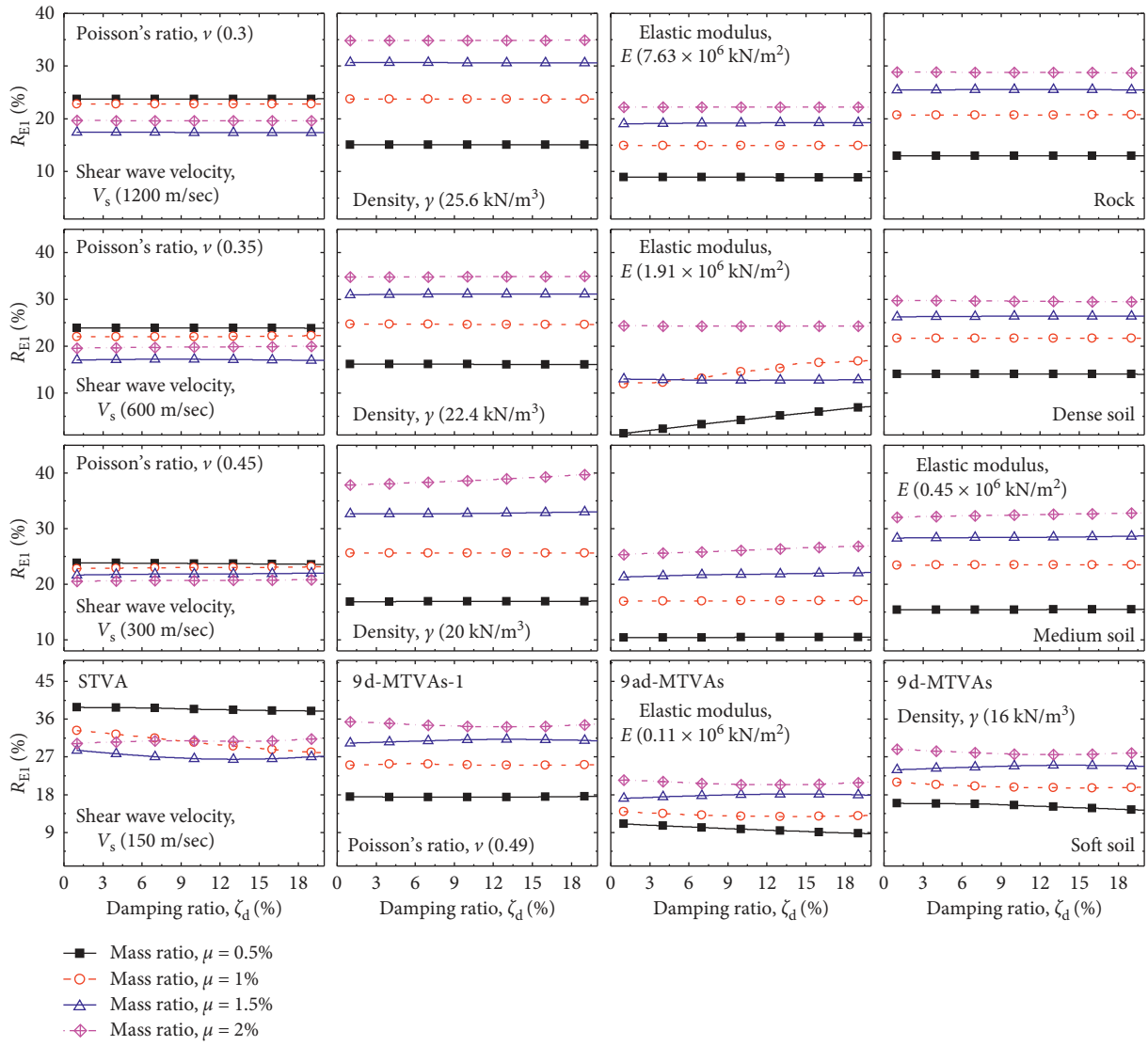

FIGURE 6: Variations of damping ratios (ζ_d) for different mass ratios (μ) of the STVA, 9d-MTVAs-1, 9ad-MTVAs, and 9d-MTVAs installed on the chimney including SSI under Llolleo (1985) earthquake ground motion.

excitations is $0.712g$ and $1.096g$, respectively. Here, g denotes gravitational acceleration. To show the effectiveness of the control schemes, the effectiveness criteria for displacement (R_{E1}) and acceleration (R_{E2}) are defined as follows:

$$R_{E1} = \left[1 - \frac{x_{20}}{X_{20}}\right] \times 100,$$
$$R_{E2} = \left[1 - \frac{\ddot{x}_{20}}{\ddot{X}_{20}}\right] \times 100, \quad (9)$$

where x_{20} and $\ddot{x}_{20}$, respectively, are the controlled peak displacement and peak acceleration at the topmost node of the chimney. Furthermore, X_{20} and $\ddot{X}_{20}$, respectively, are the uncontrolled peak displacement and peak acceleration at the topmost node of the chimney.

3.1. Effectiveness of TVA(s). The assessments between the efficiency of the four TVA schemes for seismic response mitigation of the RC chimney are presented in this section. These TVA schemes are used to control the response of the fixed-base chimney, chimney including the SSI effect. The design parameters for the TVA schemes installed on the RC chimney are provided in Table 1.

Figures 3 and 4 show the comparison between the time histories of the displacement and acceleration at the topmost node of the chimney, respectively, under Llolleo (1985) and Nahanni (1985) earthquake excitations. A time step of 0.005 sec is taken for solving the equations of motion for both Llolleo (1985) and Nahanni (1985) earthquake excitations.

In addition, the figures show the peak displacement relative to ground and peak absolute acceleration at top of the chimney for uncontrolled and controlled cases of using different configurations of the TVAs. The uncontrolled peak displacement responses of chimney with fixed base, dense soil, medium soil, and soft soil, respectively, are 0.630 m, 0.633 m, 0.640 m, and 0.660 m under Llolleo (1985) earthquake excitations. The values of the peak displacement

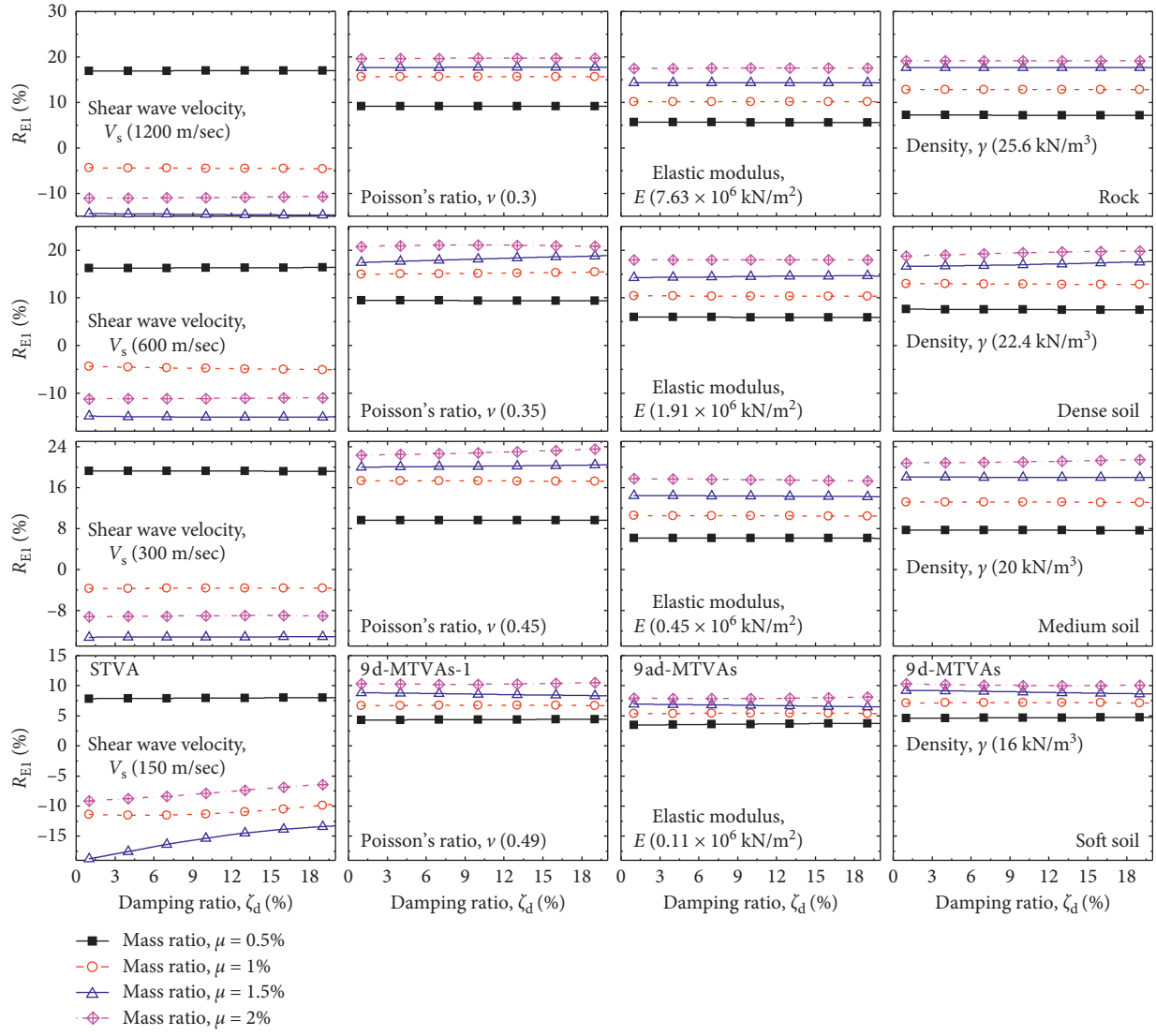

Figure 7: Variations of damping ratios (ζ_d) for different mass ratios (μ) of the STVA, 9d-MTVAs-1, 9ad-MTVAs, and 9d-MTVAs installed on the chimney including SSI under Nahanni (1985) earthquake ground motion.

response for different uncontrolled cases are 0.555 m, 0.553 m, 0.553 m, and 0.512 m under the Nahanni (1985) earthquake excitations. Similarly, the peak acceleration responses for the cases of fixed base, dense soil, medium soil, and soft soil, respectively, are $2.847g$, $2.699g$, $2.452g$, and $2.389g$ under Llolleo (1985) earthquake excitations and are $2.964g$, $2.900g$, $2.732g$, and $2.629g$ under the Nahanni (1985) earthquake excitations.

It is observed there are up to 10% variations in peak displacement response under consideration of different soil types. Furthermore, it is seen that there are up to 20% variations in peak acceleration response. Moreover, it is observed that the TVAs are effective in controlling the displacement response of the chimney in all the configurations considered herein except the STVA case. The responses of the uncontrolled chimney with different soil types are amplified by installing the STVA. Generally, from the figures, it is observed that the postpeak response (topmost node displacement) diminishes significantly when the MTVAs are added as compared to the NC and STVA cases. Similarly, it is seen that the acceleration at top of the chimney is reduced by installing different TVA schemes. The 9d-MTVAs are generally observed to have maximum reduction of top node acceleration of the chimney as compared to the STVA, 9d-MTVAs-1, and 9ad-MTVAs. Hence, it is concluded that the d-MTVAs controlling multimodal response are more consistent in efficiently mitigating the displacement and the acceleration responses.

3.2. Effect of Mass Ratio (μ) and Damping Ratio (ζ_d). In this section, the effect of the change in mass ratio (μ) and the damping ratio (ζ_d) of the STVA, 9d-MTVAs, 9ad-MTVAs, and 9d-MTVAs is studied under different earthquakes. The mass ratio (μ) is varied from 0.5% to 2% with an increment of 0.5%, and the damping ratio (ζ_d) is varied from 1% to 20% with an increment of 1%. The variations of these two reduction criteria with different mass and damping ratios are

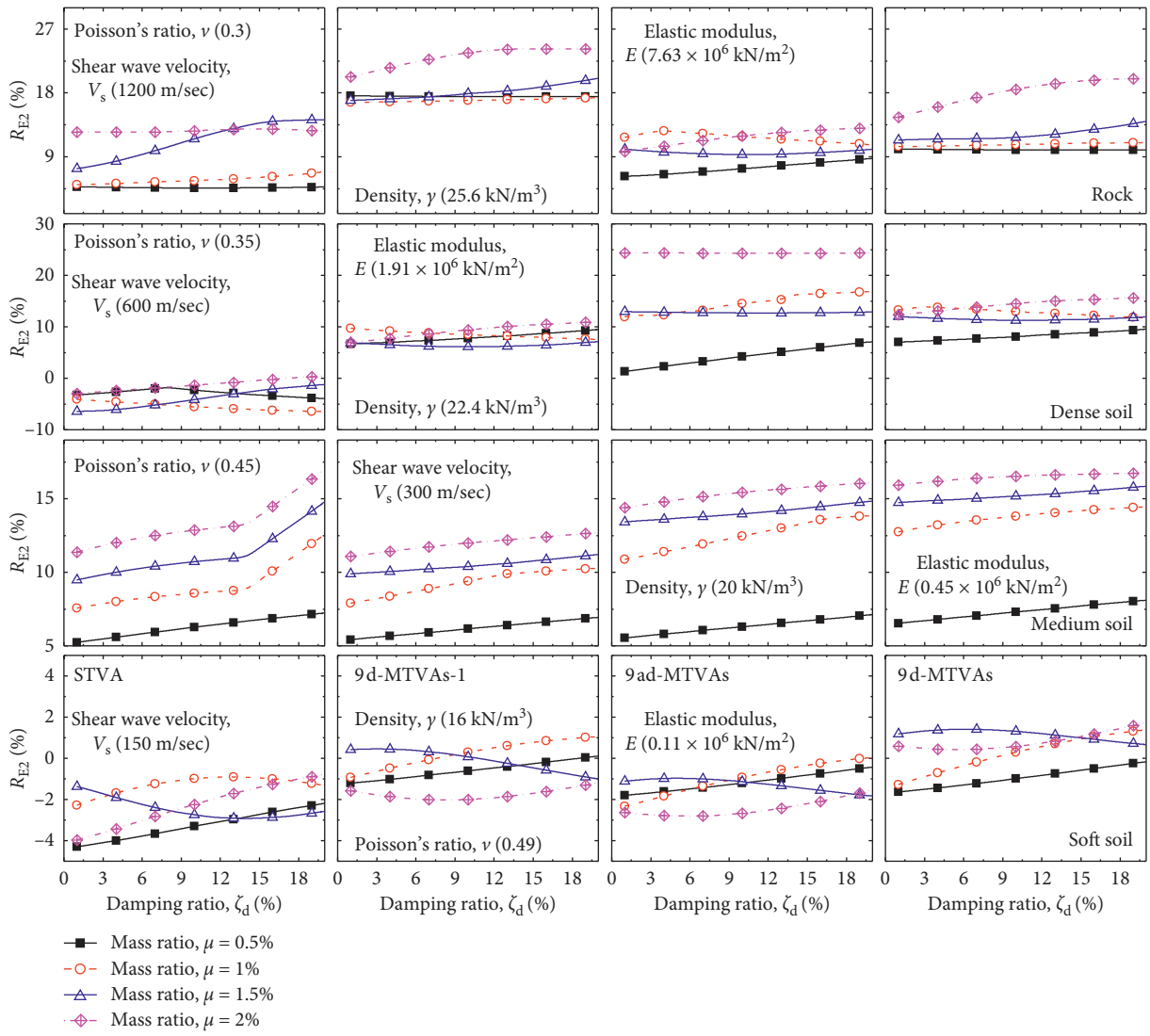

FIGURE 8: Variations of damping ratios (ζ_d) for different mass ratios (μ) of the STVA, 9d-MTVAs-1, 9ad-MTVAs, and 9d-MTVAs installed on the chimney including SSI under Llolleo (1985) earthquake ground motion.

shown in Figure 5 for the case where the chimney is fixed at the base and installed with different TVAs schemes.

It is generally observed from the figure that the pattern of variation of the reduction in responses is uniform for different types of responses and excitations for MTVAs schemes. However, it varies for the STVA scheme. Furthermore, it is seen that, in case of STVA, by increasing the mass ratio, there is significant reduction in performance of the STVA. It is due to mistuning effect of the STVA. It is seen that, for the case of STVA, optimum damping exists which could be between 5 and 8%. The better response reduction is observed by installing different MTVAs schemes. The mass ratio increased, the performance of the MTVAs schemes improved. Also, it is observed that the optimum damping ratio exists for the MTVAs schemes which is smaller as compared to the STVA scheme. Besides, it is also noticed that highest response diminution is achieved with equipment of the 9d-MTVAs as compared to STVA, 9d-MTVAs-1, and 9ad-MTVAs. Therefore, it is concluded that, by increasing the mass ratio of MTVAs schemes, the response diminution is increased as it is not the same for the STVA scheme. Figures 6–9 show the variations of damping ratios (ζ_d) for different mass ratios (μ) of the STVA, 9d-MTVAs-1, 9ad-MTVAs, and 9d-MTVAs installed on the chimney including SSI under Llolleo (1985) and Nahanni (1985) earthquake ground motions.

Four different types of soil are considered in order to compare the performance of the different TVA schemes. It is noticed that soil properties significantly condensed the efficiency of the STVA. Conversely, in MTVAs schemes, it is found that they are more robust as compared to the STVA scheme. In addition, it is noticed that the increase in damping ratios (ζ_d) may not affect the performance of the different schemes under different soil properties considered. It is mainly due to availability of the soil damping introduced to the models.

Therefore, it is concluded that the optimum damping exists for the fixed-base chimney installed with TVAs.

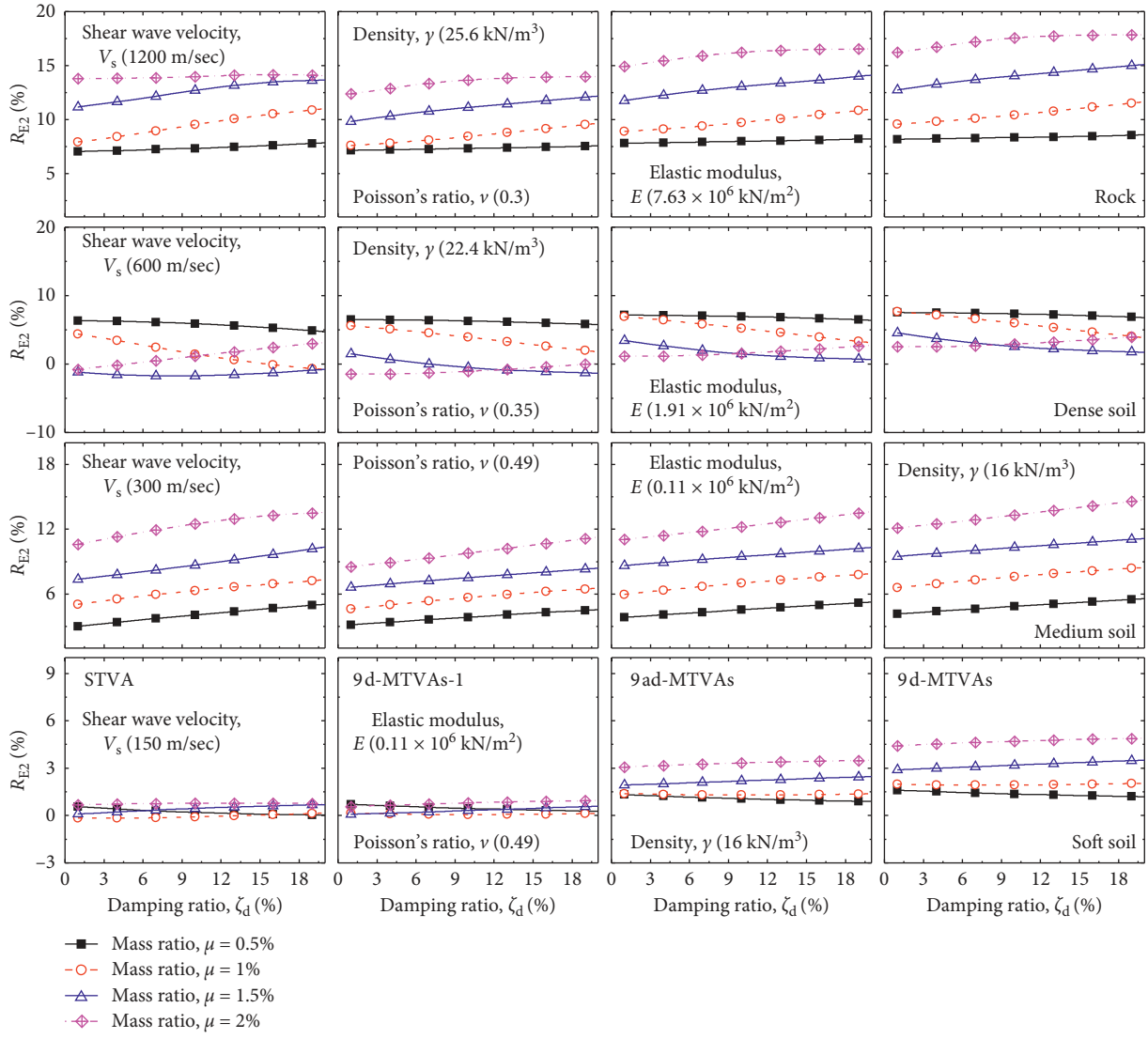

FIGURE 9: Variations of damping ratios (ζ_d) for different mass ratios (μ) of the STVA, 9d-MTVAs-1, 9ad-MTVAs, and 9d-MTVAs installed on the chimney including SSI under Nahanni (1985) earthquake ground motion.

However, damping ratios (ζ_d) may not improve the performance of the different schemes under different soil properties considered. The performance of the MTVAs schemes improved as the mass ratio increases, which is not same for the STVA scheme. Maximum displacement response control is achieved by installing d-MTVAs-1 and d-MTVAs. It is around 35 to 40% and 15 to 20% reduction in displacement response, respectively, under Llolleo (1985) and Nahanni (1985) earthquake ground motions. The d-MTVAs placed arbitrarily (ad-MTVAs) show less effectiveness as compared to the cases of d-MTVAs-1 and d-MTVAs. Yet, they are having improved performance in displacement response reduction as compared to the single TVA.

It is observed in Figures 8 and 9 that multimodal control schemes are most effective in acceleration response control as well. Generally, the best acceleration response diminution is accomplished for the chimney equipped with 9d-MTVAs. By increasing the mass ratio, increasing the control capacity of the different TVA schemes is granted. It is noticed that the acceleration response amplified as compared to the uncontrolled chimney when the chimney is equipped with the STVA and 9d-MTVAs-1 schemes.

It is also observed that the 9d-MTVAs performance is unchanged under different soil types considered herein, which means that they are more robust. Therefore, it is concluded that the increase in the mass ratio (μ) of the TVAs (i.e., masses of the units of the TVA to the mass of the chimney) leads to the increase in the seismic response reduction for most of the schemes studied herein (d-MTVAs, ad-MTVAs, and d-MTVAs). In addition, the soil type significantly influenced the design parameters of the STVA/d-MTVAs-1/ad-MTVAs/d-MTVAs schemes and seismic responses of the chimney with flexible foundation. Moreover, the d-MTVAs are more robust as compared to the STVA, d-MTVAs-1, and ad-MTVAs.

Table 1: Design parameters for the TVA schemes installed on the RC chimney.

Schemes	TVAs	Frequency, ω_i (rad/sec)	Mass, m_i (ton)	Stiffness, k_i (kN/m)	Damping, c_i (kN sec/m)
STVA	TVA-1	2.05	106.84 (2% of M_t)	447.71	3.22
9d-MTVAs-1	TVA-1	1.77	11.87	37.03	0.03
	TVA-2	1.85	11.87	40.45	0.04
	TVA-3	1.93	11.87	44.02	0.04
	TVA-4	2.00	11.87	47.27	0.04
	TVA-5	2.08	11.87	51.53	0.04
	TVA-6	2.16	11.87	55.45	0.04
	TVA-7	2.24	11.87	59.30	0.04
	TVA-8	2.31	11.87	63.61	0.05
	TVA-9	2.39	11.87	68.07	0.05
9ad-MTVAs	TVA-1	1.77	11.87	37.03	0.03
	TVA-2	1.93	11.87	44.02	0.04
	TVA-3	2.08	11.87	51.53	0.04
	TVA-4	2.25	11.87	59.83	0.04
	TVA-5	2.39	11.87	68.07	0.05
	TVA-6	6.73	11.87	536.89	0.13
	TVA-7	7.91	11.87	743.21	0.16
	TVA-8	9.10	11.87	983.00	0.18
	TVA-9	18.76	11.87	4177.14	0.37
9d-MTVAs	TVA-1	1.77	11.87	37.03	0.03
	TVA-2	1.93	11.87	44.02	0.04
	TVA-3	2.08	11.87	51.53	0.04
	TVA-4	2.25	11.87	59.83	0.04
	TVA-5	2.39	11.87	68.07	0.05
	TVA-6	6.73	11.87	536.89	0.13
	TVA-7	7.91	11.87	743.21	0.16
	TVA-8	9.10	11.87	983.00	0.18
	TVA-9	18.76	11.87	4177.14	0.37

4. Conclusions and Remarks

Multimode control of chimneys including soil-structure interaction (SSI) under earthquake ground motions is presented. Distributed multiple tuned vibration absorbers (d-MTVAs) are used for multimode control of the chimney including SSI. Assessment of seismic responses is made for the chimney equipped with a single tuned vibration absorber (STVA), the d-MTVAs all suppressing the primary modal responses (d-MTVAs-1), arbitrarily placed d-MTVAs (ad-MTVAs), and d-MTVAs under different real earthquake excitations. The following conclusions are drawn from the results of the numerical study presented here:

(1) The d-MTVAs controlling multimodal response are more consistent in efficiently mitigating the displacement and the acceleration responses.

(2) The optimum damping exists for the fixed-base chimney installed with TVAs. However, damping ratios (ζ_d) may not improve the performance of the different schemes under different soil properties considered herein.

(3) The increase in the mass ratio (μ) of the TVAs (i.e., masses of the units of the TVA to the mass of the chimney) leads to the increase in the seismic response reduction for most of the schemes studied herein (d-MTVAs, ad-MTVAs, and d-MTVAs).

(4) The soil type significantly influenced the design parameters of the STVA/d-MTVAs-1/ad-MTVAs/d-MTVAs schemes and seismic responses of the chimney with flexible foundation. Moreover, the d-MTVAs are more robust as compared to the STVA, d-MTVAs-1, and ad-MTVAs.

Data Availability

The data used to support the findings of this study are available from the corresponding author upon request.

Conflicts of Interest

The author declares that there are no conflicts of interest.

References

[1] K. C. S. Kwok and W. H. Melbourne, "Wind induced lock-in excitation of tall structures," *Journal of the Structural Division, ASCE*, vol. 107, no. 1, pp. 57–71, 1981.

[2] B. J. Vickery and A. W. Clark, "Lift or across-wind response of tapered stacks," *Journal of the Structural Division, ASCE*, vol. 90, no. 1, pp. 11–20, 1972.

[3] B. J. Watt, I. B. Boaz, J. A. Ruhl, S. A. Shipley, D. J. Dowrick, and A. Ghose, "Earthquake survivability of concrete platforms," in *Proceedings of the Conference Offshore Technology, Houston, Texas (TX), USA*, vol. 3159, pp. 957–973, May 1978.

[4] T. K. Datta and A. K. Jain, "An analytical study of the across-wind response of cylinders due to vortex shedding," *Engineering Structures*, vol. 9, no. 1, pp. 27–31, 1987.

[5] G. Solari and D. Stura, "An evaluation technique for vibration modes of structures interacting with soil," *Engineering Structures*, vol. 3, no. 4, pp. 225–232, 1981.

[6] S. Arunachalam, S. P. Govindaraju, N. Lakshmanan, and T. V. S. R. Appa Rao, "Across-wind aerodynamic parameters of tall chimneys with circular cross section-a new empirical model," *Engineering Structures*, vol. 23, no. 5, pp. 502–520, 2001.

[7] T. Chmielewski, P. Górski, B. Beirow, and J. Kretzschmar, "Theoretical and experimental free vibrations of tall industrial chimney with flexibility of soil," *Engineering Structures*, vol. 27, no. 1, pp. 25–34, 2005.

[8] A. Kareem, "Mitigation of wind induced motion of tall buildings," *Journal of Wind Engineering and Industrial Aerodynamics*, vol. 11, no. 1-3, pp. 273–284, 1983.

[9] A. M. Aly, A. Zasso, and F. Resta, "Dynamics and control of high-rise buildings under multi-directional wind loads," *Smart Materials Research, Hindawi*, vol. 2011, Article ID 549621, 2011.

[10] A. M. Aly, "Proposed robust tuned mass damper for response mitigation in buildings exposed to multidirectional wind," *The Structural Design of Tall and Special Buildings*, vol. 23, no. 9, pp. 664–691, 2012.

[11] A. M. Aly, "Vibration control of high-rise buildings for wind: a robust passive and active tuned mass damper," *Smart Structures and Systems*, vol. 13, no. 3, pp. 473–500, 2014b.

[12] A. J. Roffel and S. Narasimhan, "Extended Kalman filter for modal identification of structures equipped with a pendulum tuned mass damper," *Journal of Sound and Vibration*, vol. 333, no. 23, pp. 6038–6056, 2014.

[13] S. Elias and V. Matsagar, "Wind response control of tall buildings with a tuned mass damper," *Journal of Building Engineering*, vol. 15, pp. 51–60, 2018.

[14] R. S. Jangid, "Optimum multiple tuned mass dampers for base-excited undamped system," *Earthquake Engineering and Structural Dynamics*, vol. 28, no. 9, pp. 1041–1049, 1999.

[15] A. S. Joshi and R. S. Jangid, "Optimum parameters of multiple tuned mass dampers for base-excited damped systems," *Journal of Sound and Vibration*, vol. 202, no. 5, pp. 657–667, 1997.

[16] Z. Lu, X. Lu, W. Lu, and S. F. Masri, "Experimental studies of the effects of buffered particle dampers attached to a multi-degree-of-freedom system under dynamic loads," *Journal of Sound and Vibration*, vol. 331, no. 9, pp. 2007–2022, 2012.

[17] Z. Lu, S. F. Masri, and X. L. Lu, "Parametric studies of the performance of particle dampers under harmonic excitation," *Structural Control and Health Monitoring*, vol. 18, no. 1, pp. 79–98, 2011.

[18] T. Bandivadekar and R. Jangid, "Optimization of multiple tuned mass dampers for vibration control of system under external excitation," *Journal of Vibration and Control*, vol. 19, no. 12, pp. 1854–1871, 2012.

[19] W. Guo, H.-N. Li, G.-H. Liu, and Z.-W. Yu, "A simplified optimization strategy for nonlinear tuned mass damper in structural vibration control," *Asian Journal of Control*, vol. 14, no. 4, pp. 1059–1069, 2011.

[20] S. Elias and V. Matsagar, "Research developments in vibration control of structures using passive tuned mass dampers," *Annual Reviews in Control*, vol. 44, pp. 129–156, 2017.

[21] S. Elias, V. Matsagar, and T. K. Datta, "Effectiveness of distributed tuned mass dampers for multi-mode control of chimney under earthquakes," *Engineering Structures*, vol. 124, pp. 1–16, 2016.

[22] S. Elias, V. A. Matsagar, and T. K. Datta, "Distributed tuned mass dampers for multi- mode control of benchmark building under seismic excitations," *Journal of Earthquake Engineering*, 2017.

[23] D. Gill, S. Elias, A. Steinbrecher, C. Schröder, and V. A. Matsagar, "Robustness of multi-mode control using tuned mass dampers for seismically excited structures," *Bulletin of Earthquake Engineering*, vol. 15, no. 12, pp. 5579–5603, 2017.

[24] S. Elias, "Seismic energy assessment of buildings with tuned vibration absorbers," *Shock and Vibration*, pp. 1–10, 2018, In press.

[25] X. Tong, X. Zhao, and S. Zhao, "Load reduction of a monopile wind turbine tower using optimal tuned mass dampers," *International Journal of Control*, vol. 90, no. 7, pp. 1283–1298, 2015.

[26] C. Zaafouri, B. Torchani, A. Sellami, and G. Garcia, "Uncertain saturated discrete-time sliding mode control for A wind turbine using a two-mass model," *Asian Journal of Control*, vol. 20, no. 2, pp. 802–818, 2017.